Eur. Phys. J. A (2017) **53**: 13
DOI 10.1140/epja/i2017-12197-5

THE EUROPEAN PHYSICAL JOURNAL A

Regular Article – Experimental Physics

Hyperfine structure of electronic levels and the first measurement of the nuclear magnetic moment of ^{63}Ni

A.B. D'yachkov, V.A. Firsov, A.A. Gorkunov, A.V. Labozin, S.M. Mironov, E.E. Saperstein, S.V. Tolokonnikov, G.O. Tsvetkov[a], and V.Y. Panchenko

National Research Center "Kurchatov Institute", academician Kurchatov sq. 1, 123182 Moscow, Russia

Received: 3 November 2016 / Revised: 15 December 2016
Published online: 25 January 2017 –
Communicated by A. Jokinen

Abstract. Laser resonant photoionization spectroscopy was used to study the hyperfine structure of the optical $3d^8 4s^2\,{}^3F_4 \rightarrow 3d^8 4s4p\,{}^3G^{\rm o}{}_3$ and $3d^9 4s\,{}^3D_3 \rightarrow 3d^8 4s4p\,{}^3G^{\rm o}{}_3$ transitions of ^{63}Ni and ^{61}Ni isotopes. Experimental spectra allowed us to derive hyperfine interaction constants and determine the magnetic dipole moment of the nuclear ground state of ^{63}Ni for the first time: $\mu = +0.496(5)\mu_{\rm N}$. The value obtained agrees well with the prediction of the self-consistent theory of finite Fermi systems.

1 Introduction

Thirty-one isotopes of nickel are presently known: ^{48}Ni–^{78}Ni [1]. Among these, the stable isotopes are isotopes ^{58}Ni, ^{60}Ni, ^{61}Ni, ^{62}Ni, and ^{64}Ni with abundances of 68.07%, 26.22%, 1.14%, 3.63%, and 0.93%, respectively. The most long-lived unstable isotopes of nickel are ^{59}Ni ($\sim 8 \times 10^4$ years), ^{63}Ni ($\sim 10^2$ years), and ^{56}Ni (6 days); most of the other isotopes have lifetimes shorter than tens of seconds. The even-mass isotopes of nickel have nuclear magnetic moments in the ground state equal to zero. The magnetic moments of the odd isotopes have nonzero values which have been measured for ^{55}Ni, ^{57}Ni, ^{61}Ni, ^{65}Ni, and ^{67}Ni [2]. The magnetic moment of ^{63}Ni in the ground state has not been measured yet; only the magnetic moments for several excited nuclear states of ^{63}Ni have been defined [2–4].

The magnetic moments of nuclei have played an important role in the development of nuclear theories like the shell model [5], the theory of finite Fermi systems (TFFS) [6], and the theory of meson exchange currents [7]. The magnetic moments and other characteristics of the nickel isotopes are of particular interest because this isotopic chain is unique. Indeed, it contains three doubly magic nuclei, allowing to study the evolution of the nuclear properties when moving from one magic nucleus to another. Systematic calculations of the magnetic moments of odd spherical nuclei [8,9] on the basis of the self-consistent TFFS [10] have been performed. However, the ^{63}Ni nucleus was not considered in these calculations.

Ground-state nuclear magnetic moments in the nickel isotopic chain have been investigated by measurements of nuclear magnetic resonance (NMR) or angular distributions in the γ-emission of oriented nuclei [2]. This work aims to determine the nuclear magnetic moment of ^{63}Ni by laser spectroscopy of its hyperfine structure (HFS). Similar investigations of the HFS in atomic optical spectra have been successfully and widely used to determine the nuclear properties of stable and radioactive isotopes [11–16]. However, the HFS in the optical spectra of the nickel isotopes has not yet been explored.

The HFS of the atomic level splitting Δ_F relative to their "center of gravity" (or centroid) energy $E_{\rm c}$ is described by the constants of the magnetic dipole (A) and electric quadrupole (B) interactions and depends on the total angular momentum J of the electrons, the nuclear spin I, and the total angular momentum F of the atom [17]:

$$\Delta_F = \frac{A}{2} \cdot K + \frac{B}{4} \cdot \frac{\frac{3}{2}K(K+1) - 2I(I+1)J(J+1)}{J(2I-1)(2J-1)I}, \quad (1)$$

where $K = F(F+1) - J(J+1) - I(I+1)$; $B \neq 0$ if $I > 1/2$ and $J > 1/2$.

For every hyperfine multiplet and a pair of isotopes the relation

$$\frac{A_1}{A_2} = \frac{I_2 \cdot {\mu_I}^{(1)}}{I_1 \cdot {\mu_I}^{(2)}}(1 + \Delta_{12}) \quad (2)$$

is valid [18]; where μ_I is the magnetic dipole moment of the nucleus with spin I, and Δ_{12} is the hyperfine anomaly difference of isotopes 1 and 2. Data on the hyperfine anomaly for the nickel isotopes were not found in the literature, but in rare cases it reaches several percent; in most cases, Δ_{12}

[a] e-mail: glebtsvetkov@mail.ru

is $\sim 10^{-4}$ or less [19]. Equation (3) in the form of

$$\mu_I^{(1)} = \frac{A_1}{A_2}\frac{I_1}{I_2} \cdot \mu_I^{(2)} \tag{3}$$

can be used to determine the magnetic moment of isotope 1 (excluding the hyperfine anomaly) if the magnetic moment of isotope 2 is known. As a reference, we used the ^{61}Ni isotope, the magnetic moment of which was measured with high accuracy by NMR: $\mu_I = -0.74868(4)\mu_N$ [20]. Since the ground-state spins of ^{63}Ni ($I_1 = 1/2$) and ^{61}Ni ($I_2 = 3/2$) are known, it was necessary to define the coefficients A of both isotopes for the same multiplet.

2 Experiment

Laser resonance photoionization spectroscopy of nickel isotopes was performed using a setup consisting of a vacuum chamber with a thermal evaporator ($T \sim 1700\,^\circ$C) and a commercial quadrupole mass spectrometer (MS-7302). A diaphragm system installed above the evaporator allowed the formation of a narrow beam of nickel atoms with a divergence angle of 3° (Doppler broadening ~ 100 MHz). Atoms were photoionized through a two-step optical scheme with ionization into the continuum (the ionization threshold was 61619.77 cm^{-1}) by irradiation of a pulsed dye laser pumped by a copper vapor laser with a pump wavelength of 578 nm and repetition rate of 10 kHz. The dye laser allowed smooth wavelength scanning (without mode jumps) of the single mode radiation with a range of ~ 1 Å by changing the voltage of the piezoelectric supports of the cavity dispersive elements. The visible laser emission (cresyl violet dye, spectral linewidth of 100 MHz, pulse width of 15 ns) was converted into the UV range (316 nm) in a nonlinear crystal of β-BBO ($4 \times 4 \times 5$ mm; $\theta = 39°$, $\varphi = 90°$). The dye laser wavelength was controlled by a precision wavelength meter (LM-007). Laser light was guided in the mass spectrometer and the radiation power density in the spectrometer chamber was ≤ 50 mW/cm^2. The laser beam intersected the atomic beam directly within the mass spectrometer ion source. The directions of the laser and atomic beams were mutually orthogonal. Photoions were detected by a secondary electron multiplier. Natural metallic nickel was used in experiments with ^{61}Ni, and a ^{63}Ni sample was prepared by ZAO "RITVERTS" (Russia).

3 Results and analysis

Photoionization into the continuum was carried out through an intermediate level $3d^8 4s4p\ ^3G^o_3$ from the lower metastable level $3d^9 4s\ ^3D_3$ (Ni I 204.786 cm^{-1} with a population of 0.27 at the nickel vaporization temperature of $\sim 1700\,^\circ$C) (fig. 1); these levels are hereafter referred to as $^3G^o_3$ and $^3D_3$, respectively.

The photoion signals recorded for both isotopes while scanning the laser wavelength of the $^3D_3 \rightarrow {}^3G^o_3$ transition are shown in figs. 2 and 3. The investigation of the

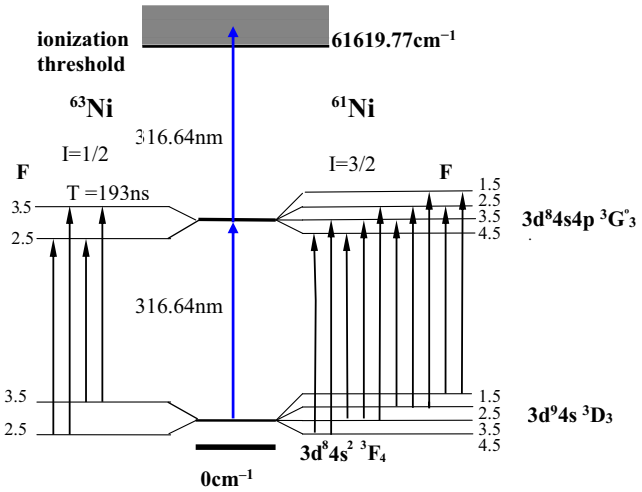

Fig. 1. Photoionization optical scheme and the hyperfine splitting (HFS) of the $^3D_3 \rightarrow {}^3G^o_3$ transitions for ^{63}Ni and ^{61}Ni. Isotope shifts of the states involved and ground-state HFS are not shown.

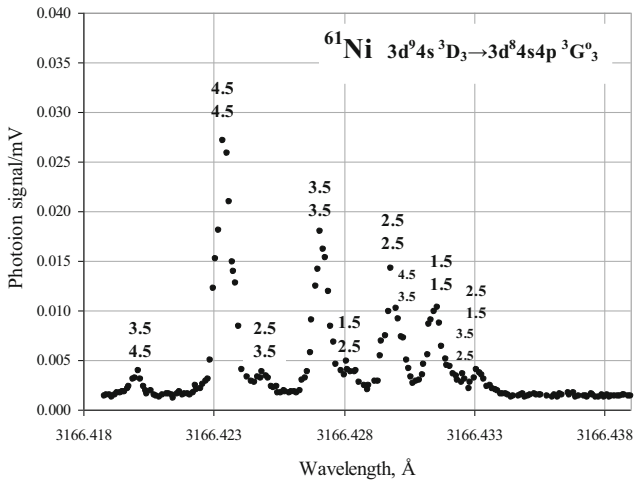

Fig. 2. The $^3D_3 \rightarrow {}^3G^o_3$ transition hyperfine spectrum of ^{61}Ni. The numbers above the peaks denote the F-values of the lower and upper states, respectively (see fig. 1). The positions of the not resolved peaks are labeled by the small font.

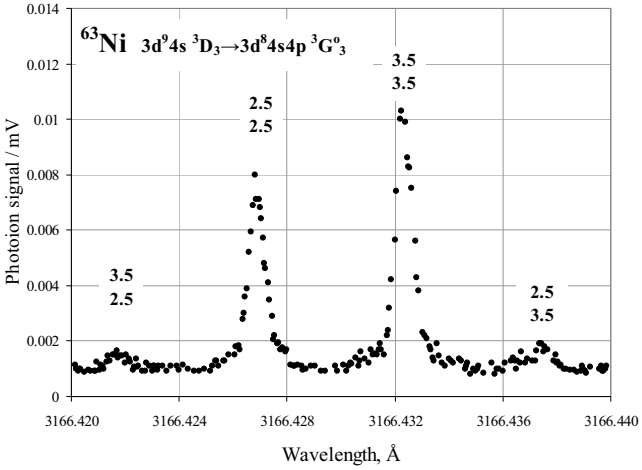

Fig. 3. Spectrum of the $^3D_3 \rightarrow {}^3G^o_3$ transition of ^{63}Ni showing hyperfine splitting. The numbers above the peaks denote the F-values of the lower and upper states (see fig. 1).

Table 1. HFS level parameters of ^{63}Ni and ^{61}Ni. The values indicated by * are from [23]. The value indicated by ** was not involved in the further calculations since it has a much larger error than in [23].

Level	$A^{(61)}$, MHz	$B^{(61)}$, MHz	$A^{(63)}$, MHz	$A^{(63)}/A^{(61)}$	E_c of ^{63}Ni, cm^{-1}
$3d^8 4s^2\,{}^3F_4$	−215.040(2)*	−56.868(18)*	429(24)	−1.99(11)	0
$3d^9 4s\,{}^3D_3$	−454.972(3)* −451(7)**	−102.951(16)* −106(30)	903(11)	−1.98(2)	204.911(1)
$3d^8 4s4p\,{}^3G^o{}_3$	−219(4)	−8(32)	446(22)[(a)] 440(11)[(b)]	−2.04(15)[(a)] −2.01(10)[(b)]	31786.218(1)

[(a)] ${}^3F_4 \rightarrow {}^3G^o{}_3$ transition.
[(b)] ${}^3D_3 \rightarrow {}^3G^o{}_3$ transition.

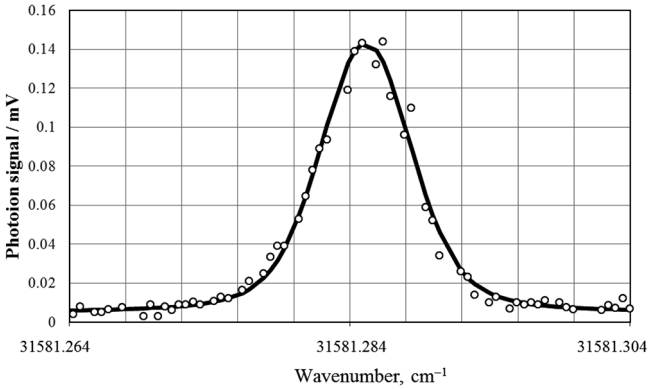

Fig. 4. Photoion current of ^{63}Ni scanning near the hyperfine line 3.5-3.5 and the result of the approximation.

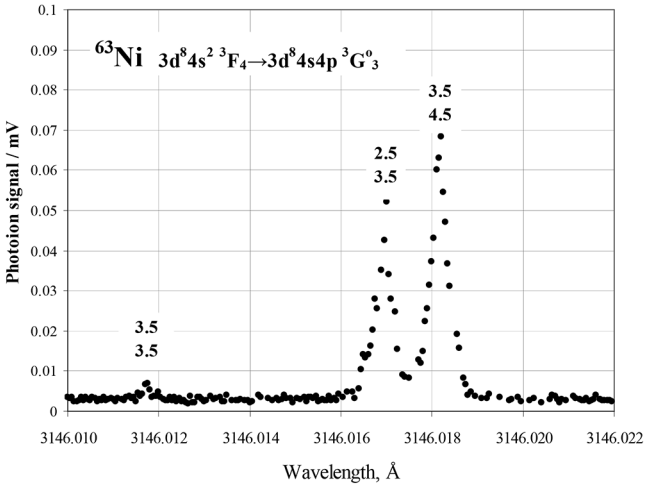

Fig. 5. Hyperfine splitting spectrum of the ${}^3F_4 \rightarrow {}^3G^o{}_3$ transition for ^{63}Ni.

HFS of each isotope was possible because of the separation of certain photoions by the quadrupole mass filter of the mass spectrometer. The HFS width of ^{61}Ni was ~ 3.95 GHz, and eight of ten lines were spectrally resolved. The ^{63}Ni HFS components were resolved completely.

The experimental data were fitted to a Voigt contour to find the peak wavelength of each resonance (fig. 4). We used the package PAW of the CERN library [21] for this purpose.

The identification of the HFS components was based on their expected relative intensity [22]. The measurement of each spectrum was carried out at nominal laser intensity and increased by five times to confirm the absence of saturation effects of the HFS patterns. Four strong peaks of ^{61}Ni (fig. 2) were identified as the 4.5-4.5, 3.5-3.5, 2.5-2.5, and 1.5-1.5 components. This allowed us to determine the constants of the level ${}^3G^o{}_3$ by means of χ^2 optimization and thereby to define the whole HFS of the transition (the ${}^3D_3$ level factors A and B known from [23] were confirmed as well). The positions of the weak not resolved resonances (3.5-4.5 and 2.5-3.5) were found to be close to 2.5-2.5 and 1.5-1.5 peaks (fig. 2) correspondingly. The effect of the small peaks on the strong peak wavelengths determination was much less than wavelength measuring accuracy. To identify the ^{63}Ni spectrum, we used the fact that the ratio of the upper- and lower-level A constants is equal for the same transition across the entire isotopic chain. This ratio for ^{61}Ni was about 0.48, and this specific value is possible for ^{63}Ni for only two combinations: the first combination identified is shown in fig. 3, and the other one corresponds to the simultaneous F substitution of weak and strong resonances: 2.5-3.5 to 3.5-2.5 and 2.5-2.5 to 3.5-3.5. This substitution gave the same absolute values for the constants A but different signs. To find out the correct sign of A, the ^{63}Ni HFS was additionally investigated for the $3d^8 4s^2\,{}^3F_4 \rightarrow 3d^8 4s4p\,{}^3G^o{}_3$ transition (fig. 5). The relative positions of the resonances indicated that the sign of A is positive; otherwise, the weak peak 3.5-3.5 would be located to the right of the strong resonances.

The results of the spectra treatment are shown in table 1. The constants of the states and the energies of the ${}^3D_3 \rightarrow {}^3G^o{}_3$ and ${}^3F_4 \rightarrow {}^3G^o{}_3$ transitions were obtained for ^{63}Ni. The presented A and B coefficients of the upper ${}^3G^o{}_3$ level of ^{61}Ni were fitted using the known constants of the lower ${}^3D_3$ level [23]. The experimental constants A and B of the ${}^3D_3$ level are given for comparison with published data.

The weighted average of the $A^{(63)}/A^{(61)}$ ratios is 1.99(2) and it was chosen for the final value. According to eq. (3), this leads to a ^{63}Ni magnetic dipole moment μ of $+0.496(5)\mu_N$.

4 Description of the magnetic moments of the odd Ni isotopes within the TFFS

In the framework of the TFFS, the magnetic moment of an odd nucleus is determined in terms of the effective field $V[\hat{\boldsymbol{\mu}}]$, where $\hat{\boldsymbol{\mu}}$ is the operator of the magnetic moment:

$$\hat{\boldsymbol{\mu}} = g_l \hat{\mathbf{l}} + \frac{1}{2} g_s \hat{\boldsymbol{\sigma}}, \tag{4}$$

with $g_l^p = 1$, $g_l^n = 0$, $g_s^p = 5.586$, and $g_s^n = -3.826$. The effective field V obeys an equation that is similar to the RPA equation with the Landau-Migdal amplitude $\mathcal{F}$ playing the role of the effective NN interaction. In systems without pairing, *e.g.*, magic nuclei, this equation reads

$$V[\hat{\boldsymbol{\mu}}] = e_q \hat{\boldsymbol{\mu}} + \mathcal{F} A V[\hat{\boldsymbol{\mu}}], \tag{5}$$

where $A = \int G(\varepsilon) G(\varepsilon) \mathrm{d}\varepsilon/(2\pi i)$ is the particle-hole propagator, and G is the Green function. The spin-dependent components of $\mathcal{F}$ participate in eq. (5), along with the tensor terms induced by the pion and ρ-meson exchange; *e.g.*, see [24,25]. The formalism and generalization of eq. (5) for superfluid nuclei, as the major part of Ni isotopes, is described in detail in [8,9]. Here we present only the explicit form of the local quasiparticle charge e_q in eq. (6) because there is some difference from its usual TFFS definition [6,25]:

$$e_q^{(0)} \hat{\boldsymbol{\mu}} = \frac{1 + (1 - 2\zeta_l)\hat{\tau}_3}{2} \hat{\mathbf{l}} + \frac{(g_s^p + g_s^n) + (g_s^p - g_s^n)(1 - 2\zeta_s)\hat{\tau}_3}{4} \hat{\boldsymbol{\sigma}}. \tag{6}$$

In refs. [8,9], a new "tensor" (or "l-forbidden") quasiparticle charge

$$e_q^{(t)} \hat{\boldsymbol{\mu}} = \zeta_t [Y_2(\mathbf{n}) \circledast \hat{\boldsymbol{\sigma}}]^1, \tag{7}$$

was added to eq. (6). Here we used the same calculation scheme as in [8,9], with one exception. The self-consistent basis of the energy density functional (EDF) method developed by Fayans and co-authors (see [26] and references therein) was used in [8,9] with the original Fayans density functional DF3. Here we used the modified EDF DF3-a developed in [27], which differs from DF3 only for the spin-orbit and tensor terms. The results for the magnetic moments μ_{th} of the ground and some excited states of the odd Ni isotopes are given in table 2, along with the known experimental data. For convenience, the Schmidt values μ_{Sch} are also provided.

The agreement of the calculated magnetic moments, with the available experimental data is rather good. The rms deviation of the theoretical predictions from the experimental data is $0.13\mu_{\mathrm{N}}$, while the maximal deviation, for ^{65}Ni, is $0.21\mu_{\mathrm{N}}$. As for the value for ^{63}Ni obtained in this work, it is reproduced by the self-consistent TFFS sufficiently well.

Table 2. Magnetic moments (in μ_{N}) of Ni isotopes. The values of μ_{exp} are taken from [2]. * indicates excited states.

Nucleus	λ	μ_{exp}	μ_{Sch}	μ_{th}
^{49}Ni	$f_{7/2}$		−1.913	−1.417
	$p^*_{3/2}$		−1.913	−1.368
	$f^*_{5/2}$		1.366	0.856
^{51}Ni	$f_{7/2}$		−1.913	−1.126
	$p^*_{3/2}$		−1.913	−1.148
	$f^*_{5/2}$		1.366	0.681
^{53}Ni	$f_{7/2}$		−1.913	−1.056
	$p^*_{3/2}$		−1.913	−1.100
	$p^*_{1/2}$		0.638	0.477
	$f^*_{5/2}$		1.366	0.638
^{55}Ni	$p_{3/2}$	±0.98(3)	−1.913	−0.982
	$f^*_{7/2}$		−1.913	−0.985
	$p^*_{1/2}$		0.638	0.463
	$f^*_{5/2}$		1.366	0.593
^{57}Ni	$p_{3/2}$	−0.7975(14)	−1.913	−0.853
	$p^*_{1/2}$		0.638	0.445
	$f^*_{5/2}$		1.366	0.537
^{59}Ni	$p_{3/2}$		−1.913	−0.938
	$p^*_{1/2}$		0.638	0.447
	$f^*_{5/2}$	0.35(15)	1.366	0.535
^{61}Ni	$p_{3/2}$	−0.74868(4)	−1.913	−0.923
	$p^*_{1/2}$		0.638	0.448
	$f^*_{5/2}$	0.480(6)	1.366	0.533
^{63}Ni	$p_{1/2}$	0.496(5) —this work	0.638	0.468
	$f^*_{5/2}$	0.752(3)	1.366	0.601
	$g^*_{9/2}$	−1.211(13)	−1.913	−1.128
^{65}Ni	$f_{5/2}$	0.69(6)	0.638	0.475
	$p^*_{1/2}$		1.366	0.625
	$g^*_{9/2}$	−1.332(14)	−1.913	−1.201
^{67}Ni	$p_{1/2}$	0.601(5)	0.638	0.486
	$f^*_{5/2}$	0.56(3)	1.366	0.670
	$g^*_{9/2}$		−1.913	−1.234
^{69}Ni	$g_{9/2}$		−1.913	−1.294
	$p^*_{1/2}$		0.638	0.495
	$f^*_{5/2}$		1.366	0.709
^{71}Ni	$(g_{9/2})$		−1.913	−1.246
	$(p^*_{1/2})$		0.638	0.487
	$f^*_{5/2}$		1.366	0.679
^{73}Ni	$g_{9/2}$		−1.913	−1.119
	$p^*_{1/2}$		0.638	0.478
	$f^*_{5/2}$		1.366	0.646
^{75}Ni	$g_{9/2}$		−1.913	−1.109
	$p^*_{1/2}$		0.638	0.466
	$f^*_{5/2}$		1.366	0.603
^{77}Ni	$g_{9/2}$		−1.913	−1.056
	$p^*_{1/2}$		0.638	0.454
	$f^*_{5/2}$		1.366	0.559

5 Conclusions

The HFS of nickel isotopes in optical spectra were investigated for the first time. This enabled us to find the hyperfine interaction constants of the levels examined and to derive the nuclear magnetic moment of ^{63}Ni, which was not known until now. The magnetic moments of the ground and some excited states of odd nickel isotopes were calculated based on the self-consistent TFFS. Theoretical predictions agree well with most of the experimental data obtained for the nuclear magnetic moments of the nickel isotopes.

We acknowledge the support from the Russian Science Foundation (Grant Nos. 16-12-10155 and 16-12-10161). This work was also partly supported by the RFBR (Grant Nos. 14-02-00107-a, 14-22-03040-ofi_m, and 16-02- 00228-a). Calculations were partially carried out at the Computer Center of Kurchatov Institute. The ^{63}Ni laser photoionization work was supported by the RFBR (Grant No. 14-29-04070-ofi_m).

References

1. `http://nndc.bnl.gov/nudat2`.
2. N.J. Stone, *Table of Nuclear Magnetic Dipole and Electric Quadrupole Moments* (IAEA Nuclear Data Section, 2014).
3. J. Bleck, R. Michaelsen, W. Ribbe, W. Zeitz, Phys. Lett. B **32**, 41 (1970).
4. W. Müller, H.H. Bertschat, H. Haas, B. Spellmeyer, W.-D. Zeitz, Phys. Rev. B **40**, 7633 (1989).
5. A. Bohr, B.R. Mottelson, *Nuclear Structure*, Vol. **1** (Benjamin, New York, 1969).
6. A.B. Migdal, *Theory of Finite Fermi Systems and Applications to Atomic Nuclei* (Wiley, New York, 1967).
7. I.S. Towner, Phys. Rep. **155**, 264 (1987).
8. I.N. Borzov, E.E. Saperstein, S.V. Tolokonnikov, Phys. At. Nucl. **71**, 469 (2008).
9. I.N. Borzov, E.E. Saperstein, S.V. Tolokonnikov, G. Neyens, N. Severijns, Eur. Phys. J. A **45**, 159 (2010).
10. V.A. Khodel, E.E. Saperstein, Phys. Rep. **92**, 183 (1982).
11. A. Jokinen, A-H. Evensen, E. Kugler, J. Lettry, H. Ravn, P. Van Duppen, N. Erdman, Y. Jading, S. Köhler, K-L. Kratz, N. Trautman, A. Wöhr, V.N. Fedoseyev, V.I. Mishin, V. Tikhonov, ISOLDE-Collaboration, Nucl. Instrum. Methods Phys. Res. B **126**, 95 (1997).
12. M.D. Seliverstov, A.N. Andreyev, N. Barré, A.E.S. Dean, H. de Witte, D.V. Fedorov, V.N. Fedoseyev, L.M. Fraile, S. Franchoo, J. Genevey, G. Huber, M. Huyse, U. Köster, P. Kunz, S.R. Lesher, B.A. Marsh, I. Mukha, B. Roussière, J. Sauvage, I. Stefanescu, K. Van de Vel, P. Van Duppen, Yu.M. Volkov, Eur. Phys. J. A **41**, 315 (2009).
13. M. Avgoulea, Yu.P. Gangrsky, K.P. Marinova, S.G. Zemlyanoi, S. Fritzsche, D. Iablonskyi, C. Barbieri, E.C. Simpson, P.D. Stevenson, J. Billowes, E.C. Simpson, P. Campbell, B. Cheal, B. Tordoff, M.L. Bissel, D.H. Forest, M.D. Gardner, G. Tungate, J. Huikari, A. Nieminen, H. Penttilä, J. Äystö, J. Phys. G **38**, 025104 (2011).
14. T.J. Procter, J. Billowes, M.L. Bissell, K. Blaum, F. C. Charlwood, B. Cheal, K.T. Flanagan, D.H. Forest, S. Fritzsche, Ch. Geppert, H. Heylen, M. Kowalska, K. Kreim, A. Krieger, J. Krämer, K.M. Lynch, E. Mané, I.D. Moore, R. Neugart, G. Neyens, W. Nörtershäuser, J. Papuga, M.M. Rajabali, H.H. Stroke, P. Vingerhoets, D.T. Yordanov, M. Žáková, Phys. Rev. C **86**, 034329 (2012).
15. J. Papuga, M.L. Bissell, K. Kreim, C. Barbieri, K. Blaum, M. De Rydt, T. Duguet, R.F. Garcia Ruiz, H. Heylen, M. Kowalska, R. Neugart, G. Neyens, W. Nörtershäuser, M.M. Rajabali, R. Sánchez, N. Smirnova, V. Somà, D.T. Yordanov, Phys. Rev. C **90**, 034321 (2014).
16. H. Heylen, C. Babcock, J. Billowes, M.L. Bissell, K. Blaum, P. Campbell, B. Cheal, R.F. Garcia Ruiz, Ch. Geppert, W. Gins, M. Kowalska, K. Kreim, S.M. Lenzi, I.D. Moore, R. Neugart, G. Neyens, W. Nörtershäuser, J. Papuga, D.T. Yordanov, Phys. Rev. C **92**, 044311 (2015).
17. I. Sobelman, *Introduction to Theory of Atomic Spectra* (Nauka, Moscow, 1977).
18. B. Cheal, K.T Flanagan, J. Phys. G **37**, 113101 (2010).
19. J.R. Persson, At. Data Nucl. Data Tables **99**, 62 (2013).
20. L.E. Drain, Phys. Lett. **11**, 114 (1964).
21. `http://cernlibweb.cern.ch/cernlib`.
22. O. Axner, J. Gustafsson, N. Omenetto, J.D. Winefordner, Spectrochim. Acta Part B **59**, 1 (2004).
23. W.J. Childs, L.S Goodman, Phys. Rev. **170**, 136 (1968).
24. A.B. Migdal, *Theory of Finite Fermi Systems and Applications to Atomic Nuclei*, 2nd edition (Nauka, Moscow, 1983).
25. A.B. Migdal, E.E. Saperstein, M.A. Troitsky, D.N. Voskresensky, Phys. Rep. **192**, 179 (1990).
26. S.A. Fayans, S.V. Tolokonnikov, E.L. Trykov, D. Zawischa, Nucl. Phys. A **676**, 49 (2000).
27. S.V. Tolokonnikov, E.E. Saperstein, Phys. At. Nucl. **73**, 1684 (2010).